Available online at www.sciencedirect.com
SCIENCE DIRECT®
Nonlinear Analysis
Real World Applications
ELSEVIER
Nonlinear Analysis: Real World Applications 7 (2006) 81–95
www.elsevier.com/locate/na

Chaotic motions and fractal basin boundaries in spring-pendulum system

Aria Alasty*, Rasool Shabani

Center of Excellence in Design, Robotics, and Automation (CEDRA), Department of Mechanical Engineering, Sharif University of Technology, Tehran 1458889694, Iran

Received 27 June 2004; accepted 12 January 2005

Abstract

This study investigates the chaotic response of the spring-pendulum system. In this system besides of strange attractors, multiple regular attractors may co-exist for some values of system parameters, and it is important to study the global behavior of the system using the basin boundaries of the attractors. Here multiple scales method is used to distinguish the regions of stable and unstable attractors. Early studies show that there are unstable regions for the spring-pendulum system. In this study using bifurcation diagrams and Poincaré maps, it is shown that in some cases the response becomes quasi-periodic or chaotic for some deviations from external and internal resonance frequencies. Also it will be shown that the response is sensitive to the value of damping parameters, which may result in chaotic response. Results show that the jumping phenomena may occur when multiple regular attractors exist. Using basin boundaries of attractors it is also shown that in some regions these boundaries are fractal.

Keywords: Spring-pendulum system; Chaos; Jumping phenomenon; Fractal basin

1. Introduction

In many nonlinear dissipative dynamical systems, after driving the equations of motion, one usually tries to locate all possible equilibrium states and periodic solutions of the system and specify the stability of these solutions. Also for multiple solutions, evolution of the solution due to variations in system parameters or initial conditions would be important. In

* Corresponding author. Tel.: +98 21 616 5504; fax: 98 21 600 0021.
E-mail addresses: aalasti@sharif.edu (A. Alasty), shabani@mehr.sharif.edu (R. Shabani).

1468-1218/$ - see front matter © 2005 Elsevier Ltd. All rights reserved.
doi:10.1016/j.nonrwa.2005.01.003

recent years strange attractors have been found in many nonlinear dynamical systems, so one must examine the probability of chaos when the system is nonlinear. In many applications chaotic response is undesirable, because even small perturbations may cause trajectories to diverge exponentially. Therefore obtaining a limit for the parameters which introduces the chaotic response is important. Also from the practical point of view, it is important to know that what initial disturbances can trigger chaotic response. For multiple non-chaotic attractors there may be fractal boundaries between basin boundaries. This would imply that for some small uncertainties in the initial conditions near to this boundary, prediction might be impossible even if a unique solution is proved to exist.

In this paper the global behavior of a harmonically excited spring-pendulum system with internal and external resonance is investigated. The behavior of such system can be very complex when $\omega_1 \approx 2\omega_2$, and when ω_1 or $\omega_2 \approx \Omega$, where Ω, ω_1 and ω_2 denote, respectively, the forcing frequency and the linearized natural frequencies in the spring and pendulum modes. Many investigators have studied the nonlinear dynamics and chaotic solutions of multi-degree-of-freedom systems in resonance condition. Subharmonic resonance of 2DOF system with cubic nonlinearities to multi-frequency parametric excitations in the presence of 3:1 internal resonance have been investigated by El Bassiouny [4]. Quadratically coupled oscillators with 1:2 internal resonances [12], cubic nonlinear oscillators with 1:3 internal resonances [22], parametrically excited oscillators [5,14,21], quadratic nonlinear oscillators with three mode interactions [15], and also nonlinear behavior of spring pendulum [2,6,23] have been studied. Sethna used the averaging method to study a forced pendulum system ($\Omega = \omega_2$) consisting of two masses connected by a spring [20], and found jumping and amplitude-modulated motions. Nayfeh et al. used the method of multiple scales to study the nonlinear coupling of pitch and roll modes in ship motion [18]. They found jumping, amplitude-modulated motions and saturation (in pitch mode) with variation of the amplitude of pitch mode. Also Nayfeh and co-workers reported experimentally observed chaos in coupled oscillators [16,19,17]. Lee and Hsu investigated periodic solutions of spring-pendulum system using the harmonic balance method. They found that the system can have two stable steady state periodic solutions [9] and obtained domains of attractions using interpolated mapping method. Lee and Park studied chaotic solutions of spring-pendulum system and compared the response of original and approximate system. They used the method of multiple scales and considered an internal resonance condition ($\omega_1 \approx 2\omega_2$) and two external resonance conditions ($\Omega = \omega_1$ and $\Omega = \omega_2$) [10].

In a series of papers, Grebogi et al. presented numerical evidence for fractal boundaries between basins of attraction for non-chaotic attractors [7,8]. Chaotic response and boundary crises in a suspension model have been investigated by Defreitas et al. [3]. They found that the system may have both periodic and chaotic solutions, with a highly involved basins of attraction structure. Also the fractal structures of basin boundaries in two-dimensional maps have been shown in [1]. Moon and Li found fractal basin boundaries for two and three well potential oscillators [11,13] and concluded that the small uncertainties in initial conditions can lead to unpredictability of system output even when the motion is not chaotic.

In this paper the forced motion of spring pendulum system in the neighborhood of static equilibrium is studied. Using four-dimensional state equations in amplitude and phase variables, developed by the method of multiple scales [10], the effects of internal and external detuning parameters with various damping coefficients on the response of the

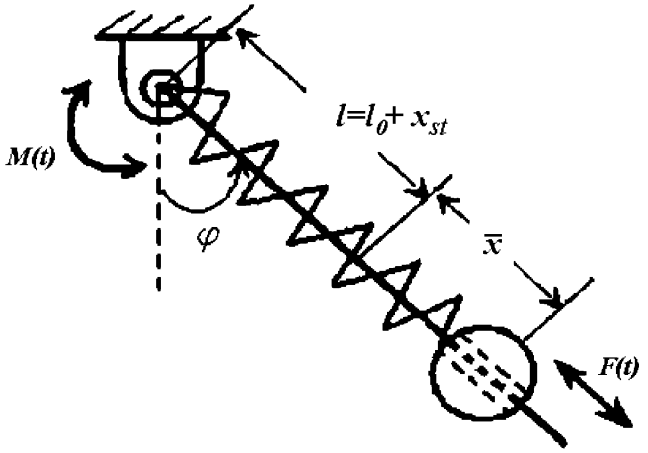

Fig. 1. Model of spring-pendulum system.

system are investigated. It is shown that for each of spring and pendulum modes with change in the external detuning parameter the number of equilibrium states is at most three and at least one. Where change in the internal resonance detuning parameter results in always one equilibrium state with no jumping. Numerical integration and tracing the long-term behavior in unstable regions is used to determine the type of the attractors. By constructing the bifurcation diagram and the Poincaré map, the chaotic and quasi-periodic motions are studied for narrow bound of system parameters. For regular response with two steady state solutions, numerical simulation is carried out to construct the basin boundaries, which show fractal boundaries.

2. Equations of motion

Consider the planar motion of a mass, m, attached to the end of a massless linear spring with stiffness k and unstretched length of l_0 (Fig. 1). The variables x and φ are the spring extensional and pendulum angular motions, respectively. A harmonic moment $M(t)$ and force $F(t)$ with angular frequency of Ω are applied to the system. Linear viscous damping forces with coefficients $\bar{c}_1$ and $\bar{c}_2$ are considered to be presented in both spring and pendulum modes, respectively. For this system the equations of motion are

$$\begin{aligned} &\ddot{x} + c_1\dot{x} + \omega_1^2 x - (1+x)\dot{\varphi}^2 + \omega_2^2(1-\cos\varphi) = f_1\cos(\Omega t) = F(t),\\ &(1+x)^2\ddot{\varphi} + c_2\dot{\varphi} + 2(1+x)\dot{x}\dot{\varphi} + \omega_2^2(1+x)\sin\varphi = f_2\cos(\Omega t) = M(t) \end{aligned} \tag{1}$$

with

$$\begin{aligned} &f_1 = F_0/ml; \quad \omega_1^2 = k/m; \quad c_1 = \bar{c}_1/m; \quad x = \bar{x}/l,\\ &f_2 = M_0/ml^2; \quad \omega_2^2 = g/l; \quad c_2 = \bar{c}_2/ml; \quad l = l_0 + mg/k, \end{aligned} \tag{2}$$

where l is the statically stretched length of spring, ω_1 and ω_2 are the linearized natural frequencies of spring and pendulum modes, respectively, and F_0 and M_0 are force and moment amplitudes. Motions are considered in the vicinity of the static equilibrium position and so we let ε be a measure of amplitude of the response and consider it to be small compared to unity. Also assume that the viscous damping forces and the amplitude of exciting force and moment are on the order of ε^2.

$$c_n = \varepsilon^2 \hat{c}_n; \quad f_n = \varepsilon^2 \hat{f}_n, \quad n = 1, 2. \tag{3}$$

To study the system response near to internal resonance ($2\omega_2 = \omega_1$) and external resonance $\Omega = \omega_s$ ($s = 1, 2$), we introduce σ_1 and σ_2 as follows:

$$2\omega_2 = \omega_1 + \varepsilon\hat{\sigma}_1 = \omega_1 + \sigma_1,$$

$$\Omega = \omega_s + \varepsilon\hat{\sigma}_2 = \omega_s + \sigma_2, \tag{4}$$

where σ_1 and σ_2 denote the internal and external detuning parameters in rad/s. In Eqs. (2)–(4) all parameters ω_1, ω_2, $\hat{c}_1$, $\hat{c}_2$, $\hat{f}_1$, $\hat{f}_2$, $\hat{\sigma}_1$, $\hat{\sigma}_2$ and Ω have the same order of magnitude equal to one.

3. Perturbation analysis

The method of multiple scales is used to obtain a uniformly valid asymptotic expansion of the solution for Eqs. (1). According to this method the different time scales defined as

$$T_n = \varepsilon^n t, \quad n = 0, 1, 2, \ldots . \tag{5}$$

The T_0 scale is associated with the relatively rapid oscillations occurring with the frequencies ω_1 and ω_2 approximately (fast scale) and the T_n ($n \geqslant 1$) are associated with the relatively slow changes in amplitudes and frequencies (slow scales). We assume that x and φ have expansion of the form

$$x(t : \varepsilon) = \varepsilon x_1(T_0, T_1) + \varepsilon^2 x_2(T_0, T_1) + \cdots,$$

$$\varphi(t : \varepsilon) = \varepsilon\varphi_1(T_0, T_1) + \varepsilon^2\varphi_2(T_0, T_1) + \cdots . \tag{6}$$

Also the derivatives are transformed according to

$$\mathrm{d}/\mathrm{d}t = D_0 + \varepsilon D_1 + \varepsilon^2 D_2 + \cdots,$$

$$\mathrm{d}^2/\mathrm{d}t^2 = D_0^2 + 2\varepsilon D_0 D_1 + \varepsilon^2(D_1^2 + 2D_0 D_2) + \cdots, \tag{7}$$

where $D_n = \partial/\partial T_n$ with substitution of Eqs. (6) and (7) into Eqs. (1) and equating coefficients of equal powers of ε we obtain two sets of equations. In this study we use the solution given by Lee and Park [10]. The solution consists of the two parts, the spring mode excitation and the pendulum mode excitation.

3.1. Spring mode excitation: ($\Omega \approx \omega_1$, $f_2 = 0$)

If a_i and γ_i $(i = 1, 2)$ denote the steady state non-dimensionalized amplitudes and phase variables of modes, thus the response of spring and pendulum modes may be obtained as

$$x = a_1 \cos(\Omega t - \gamma_1),$$
$$\varphi = a_2 \cos[\Omega t/2 - (\gamma_1 - \gamma_2)/2]. \tag{8}$$

For the steady state response of the system, two cases may be recognized:

Case (I)

$$a_2 = 0; \quad a_1 = \frac{f_1}{\omega_1\sqrt{4\sigma_2^2 + c_1^2}}; \quad \gamma_1 = \sin^{-1}\left(\frac{c_1}{\sqrt{4\sigma_2^2 + c_1^2}}\right) \tag{9}$$

and γ_2 is indeterminate.

Case (II)

$$a_1 = \frac{\sqrt{(\sigma_2 - \sigma_1)^2 + c_2^2}}{(2\omega_1 - \omega_2)/2}; \quad (a_2^2)^2 - 2\Lambda_1 a_2^2 + \Lambda_0 = 0,$$
$$\gamma_1 = \sin^{-1}\left\{\frac{\omega_1}{f_1}\left[c_1 a_1 + \frac{3\omega_2^2}{4\omega_1} a_2^2 \sin(\gamma_2)\right]\right\}; \quad \gamma_2 = \sin^{-1}\left\{\frac{c_2}{\sqrt{(\sigma_2 - \sigma_1)^2 + c_2^2}}\right\}, \tag{10}$$
$$\Lambda_0 = \frac{16(4\sigma_2^2 + c_1^2)(a_1^2 - [f_1/\sqrt{\omega_1^2(4\sigma_2^2 + c_1^2)}]}{(3\omega_2^2/\omega_1)^2}; \quad \Lambda_1 = \frac{4[2\sigma_2(\sigma_2 - \sigma_1) - c_1 c_2]}{[(3\omega_2^2/\omega_1)(2\omega_1 - \omega_2/2)]}.$$

Case (I) is the solution to the linearized problem. In this case only the spring mode responds to the excitation. Case (II) shows a quite different behavior. For this case it maybe concluded from Eqs. (10) that a_1 is independent of f_1, while a_2 depends on it. This occurs in spite of the fact that the external excitation is applied to the spring mode.

Next we determine the situations in which Eqs. (10) have real roots. It is seen that there are two real solutions for a_2:

$$a_2 = \sqrt{\Lambda_1 \pm \sqrt{\Lambda_1^2 - \Lambda_0}} \quad \text{when } \sqrt{|\Lambda_0|} < \Lambda_1 \ \& \ \Lambda_0 > 0 \tag{11}$$

and there is one real solution as

$$\left(a_{22} = \sqrt{\Lambda_1 + \sqrt{\Lambda_1^2 - \Lambda_0}}\right) \quad \text{when } \Lambda_0 < 0. \tag{12}$$

It is also seen that when $\Lambda_0 < 0$, there can be at most one real solution for a_2 and this occurs only if $\Lambda_0 < 0$, as in Eq. (12). It should be mentioned that when $0 < \Lambda_1 < \sqrt{|\Lambda_0|}$, then

Eq. (10) has no real solution for a_2, and therefore case (II) is not valid. In this situation the response of system is given by Eq. (9) of case (I). To determine that which solution gives the response, stability of various solutions should be considered. This is performed using first method of Lyapunov stability analysis. By checking all eigenvalues of Jacobian matrix in real roots of Eqs. (9) and (10), if the real parts of all four eigenvalues are negative then the solution is considered to be stable.

3.2. Pendulum mode excitation: ($\Omega \approx \omega_2$, $f_1 = 0$)

In this case consider the condition in which excitation frequency is close to ω_2. The steady state amplitude and phase variables will be [10]

$$a_1^3 + \Lambda_1 a_1^2 + \Lambda_2 a_1 + \Lambda_3 = 0; \quad \Lambda_1 = -\frac{4[4\sigma_2(2\sigma_2+\sigma_1) - c_1c_2]}{(2\omega_1-\omega_2)\sqrt{4(2\sigma_2-\sigma_1)^2 + c_1^2}},$$

$$\Lambda_2 = \frac{4(4\sigma_2^2 + c_2^2)}{(2\omega_1-\omega_2)^2}; \quad \Lambda_3 = \frac{3f_2^2}{\omega_1(2\omega_1-\omega_2)\sqrt{4(2\sigma_2-\sigma_1)^2 + c_1^2}},$$

$$a_2^2 = \frac{4\omega_1 a_1}{3\omega_2^2}\sqrt{4(2\sigma_2+\sigma_1)^2 + c_1^2},$$

$$\gamma_1 = \sin^{-1}\left\{\frac{1}{f_2}\left[\omega_2 c_2 a_2 + \frac{2\omega_1 c_1 a_1^2}{3\omega_2 a_2}(2\omega_1-\omega_2)\right]\right\}; \quad \gamma_2 = \sin^{-1}\left\{-\frac{4\omega_1 c_1 a_1}{3\omega_2^2 a_2^2}\right\}, \tag{13}$$

where the response in the spring and pendulum modes are

$$x = a_1 \cos(2\Omega t - \gamma_2 - 2\gamma_1),$$

$$\varphi = a_2 \cos(\Omega t - \gamma_2). \tag{14}$$

In this case multiple solutions exist for a_1 and a_2 while neither of them can be zero. This will be seen clearly in the numerical examples.

4. Numerical results

4.1. Spring mode excitation: ($\Omega \approx \omega_1$, $f_2 = 0$)

For $\omega_1 = 1$ and $f_1 = 0.0055$ we study the evolution of the solution (a_1 and a_2) as a function of the detuning parameters (σ_1 and σ_2) and the damping coefficients (c_1 and c_2). In Fig. 2a, a_1 and a_2 are plotted as functions of σ_2, where $\sigma_1 = -0.3$ and $c_1 = c_2 = 0.005$. The jumping phenomena associated with each mode are indicated by arrows. As σ_2 increases, a_2 moves toward B and then moves along BDE, and then it jumps down from E to F. As σ_2 decreases, a_2 solution moves along GFL and then jumps up from L to M. On the other

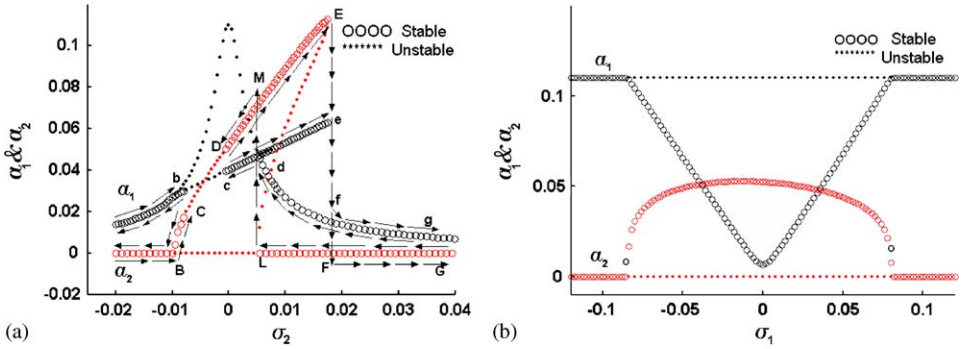

Fig. 2. Variations of steady state non-dimensionalized amplitudes of spring 'a_1' and pendulum 'a_2' modes. (a) versus σ_2 for $\sigma_1 = -0.03$ (b) versus σ_1 for $\sigma_2 = 0$.

hand, by increasing σ_2, a_1 moves toward 'e' and then jumps down from'e' to 'f' and then follows the 'fg' branch.

For a special case of ($\sigma_1 = -0.03$) note that, if σ_2 decreases, a_1 moves along the branch 'gdcb' and no jump occurs. The periodic solution of spring-pendulum system was investigated by the use of Harmonic balance method in [9], and then for a special case of $\sigma_1 = 0$ the results were evaluated. In Fig. 2b, a_1 and a_2 are plotted as functions of σ_1 for $\sigma_2 = 0$ and $c_1 = c_2 = 0.005$. For this case no jump was seen for a_1 and a_2. In Fig. 2, it is observed that for various values of σ_1 and σ_2, a minimum of one and a maximum of two stable solutions exist for a_1 and a_2.

The variations of a_1 and a_2 versus σ_2 are plotted in Fig. 3a where internal detuning parameter has been changed from -0.03 to 0.03. Based on Figs. 2a and 3a the negative or positive values of σ_1 bend the frequency response to the right (hard spring) or to the left (soft spring), respectively. Deviation from external resonance condition is shown in Fig. 3d, where a_1 and a_2 are plotted as functions of σ_1 at $\sigma_2 = 0.004$. In contrast to Fig. 2b, in Fig. 3d, a_2 jumps up from B to C when σ_1 increases and jumps down from G to A for decreasing σ_1, and a_1 also jumps down from 'g' to 'a'.

The periodic solutions are unstable in some regions (Fig. 3a, and d). Bifurcation diagrams of x and φ reveal that these unstable solutions are bounded but not periodic (Fig. 3b, c and e, f). Also variations of σ_1 and σ_2 result in period doubling phenomena for the pendulum mode. The non-periodic solutions also studied by the Poincaré map (Fig. 4a and b). The results illustrate that at the onset of instability regions the solution is chaotic. Near the boundaries of unstable regions the responses are quasi-periodic (Poincaré map of these cases are not shown here).

In Fig. 5a, a_1 is plotted as a function of σ_2 for various value of σ_1. The curve with the peak at $\sigma_2 = 0$ corresponds to $a_2 = 0$ and hence is the solution of linearized problem. The spread of unstable portion of these curves is controlled by the values of σ_1 and σ_2. Hence at a given value of σ_2, the curve may present both a stable and an unstable solution, depending on the value of σ_1. Similar plots for a_2 are given in Fig. 5b.

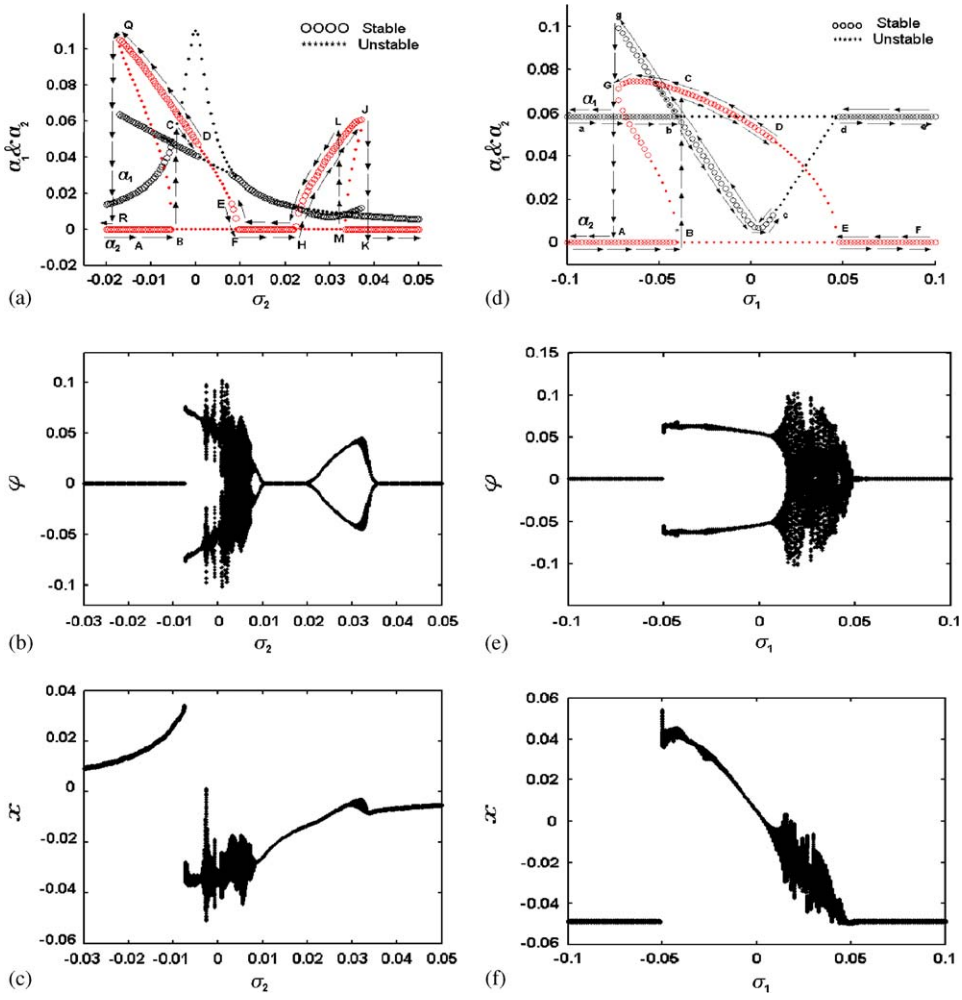

Fig. 3. Frequency responses of spring and pendulum modes and associated bifurcation diagrams. (a) Variations of a_1 and a_2 versus σ_2 for $\sigma_1 = 0.03$. (b and c) Bifurcation diagrams of φ and x associated with '(a)'. (d) Variations of a_1 and a_2 versus σ_1 for $\sigma_2 = 0.004$. (e and f) Bifurcation diagrams of φ and x associated with '(d)'.

Fig. 6a and b shows the influence of damping coefficients on the solution. It should be noted that the existence of multiple solution depends on the damping value of each modes. For special values of damping coefficients the jumping phenomena occurred.

Co-existence of multiple attractors necessitates the study of qualitative long-term behavior of state variables, describing spring-pendulum motion in presence of uncertainties in initial conditions. When the multiple attractors are detected, the initial point X_0 determines which of the specific attractors will be reached by the orbits of the state variables.

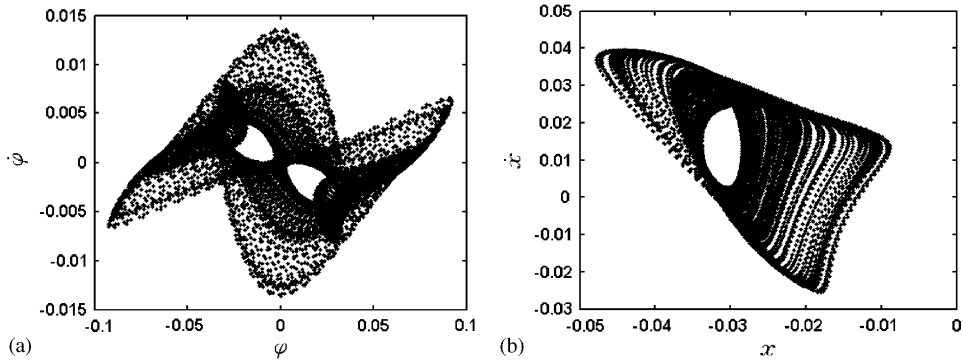

Fig. 4. Poincaré maps for $\sigma_1 = 0.03$, $\sigma_2 = 0.005$, $c_1 = c_2 = 0.005$. (a) Pendulum mode. (b) Spring mode.

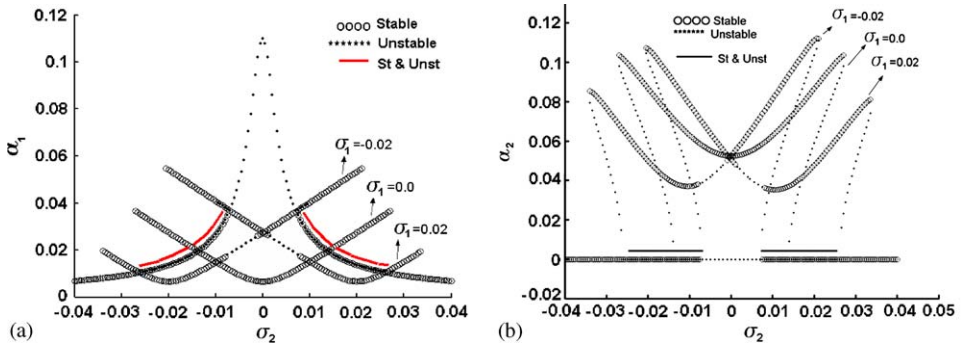

Fig. 5. (a) Spring mode amplitude and (b) pendulum mode amplitude for various value of internal detuning parameter.

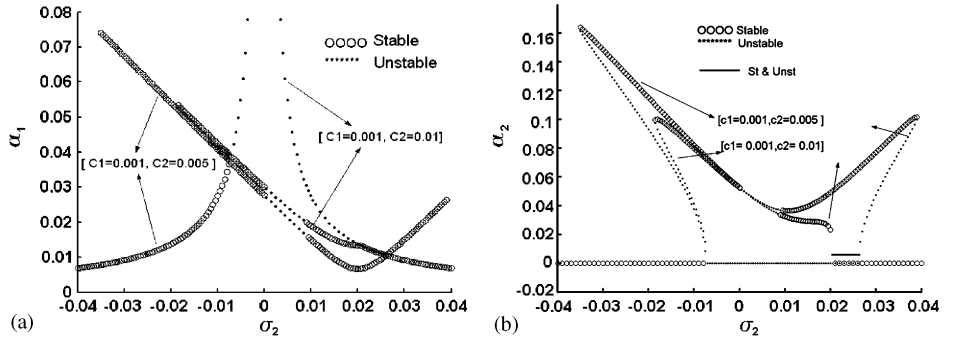

Fig. 6. (a) Spring mode amplitude and (b) pendulum mode amplitude for various values of the damping coefficients.

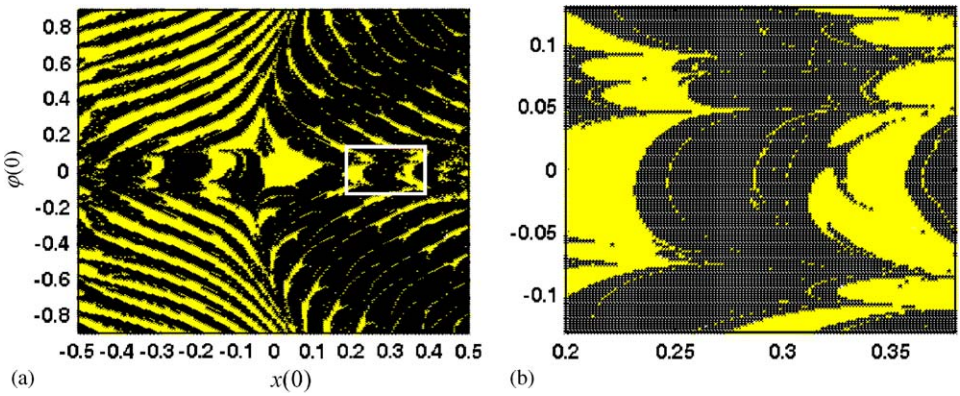

Fig. 7. Basin of attraction diagrams. (a) In $(x(0), \phi(0))$ plane and (b) Magnification of the region defined by the rectangle in '(a)'.

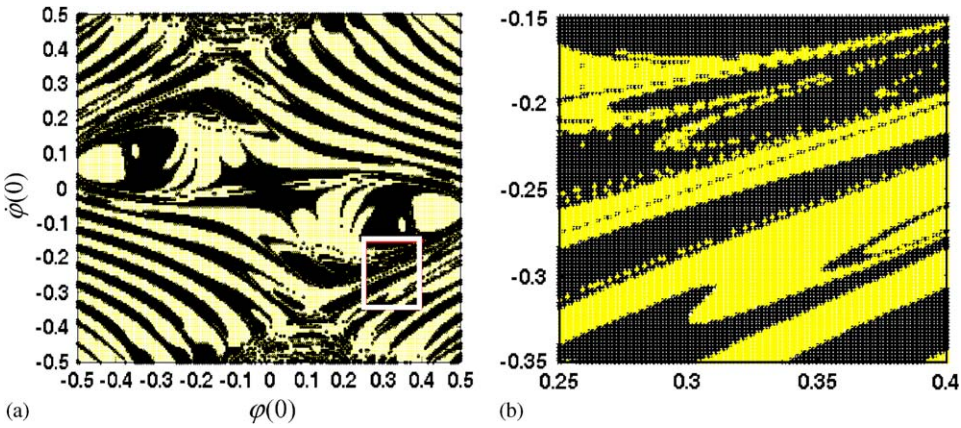

Fig. 8. Basin of attraction diagrams. (a) In $(\phi(0), \dot{\phi}(0))$ plane and (b) Magnification of the region defined by the rectangle in '(a)'.

In this system the multiple attractors are shown for specific values of parameters (Figs. 2 and 3). For example Fig. 3a shows that two stable regular attractors can be detected for pendulum mode in the range of $(-0.02 < \sigma_2 < -0.005)$. If we consider the case of $\sigma_2 = -0.01$ then the stable attractors are at $a_2 = 0$ and 0.082. For these two attractors, the projections of basin of attraction on the $(x(0), \varphi(0))$ plane is shown in Fig. 7a, for $\dot{x}(0) = -0.04$, $\dot{\varphi}(0) = 0.02$, and by discretizing the $[-0.5, 0.5] \times [-0.5, 0.5]$ square into a 200×200 grid. The black and gray regions direct the state towards $a_2 = 0.082$ and $a_2 = 0$, respectively. Some regions of this basins exhibit more intricate patterns found in fractal objects. Magnification of the projection window in Fig. 7b, also illustrates the self-similarity property of the fractal boundary. In Fig. 8a, similar basins for the same attractors are constructed in $(\dot{\varphi}(0), \varphi(0))$ plane, for: $x(0) = 0.02$, $\dot{x}(0) = -0.04$. Some portions of

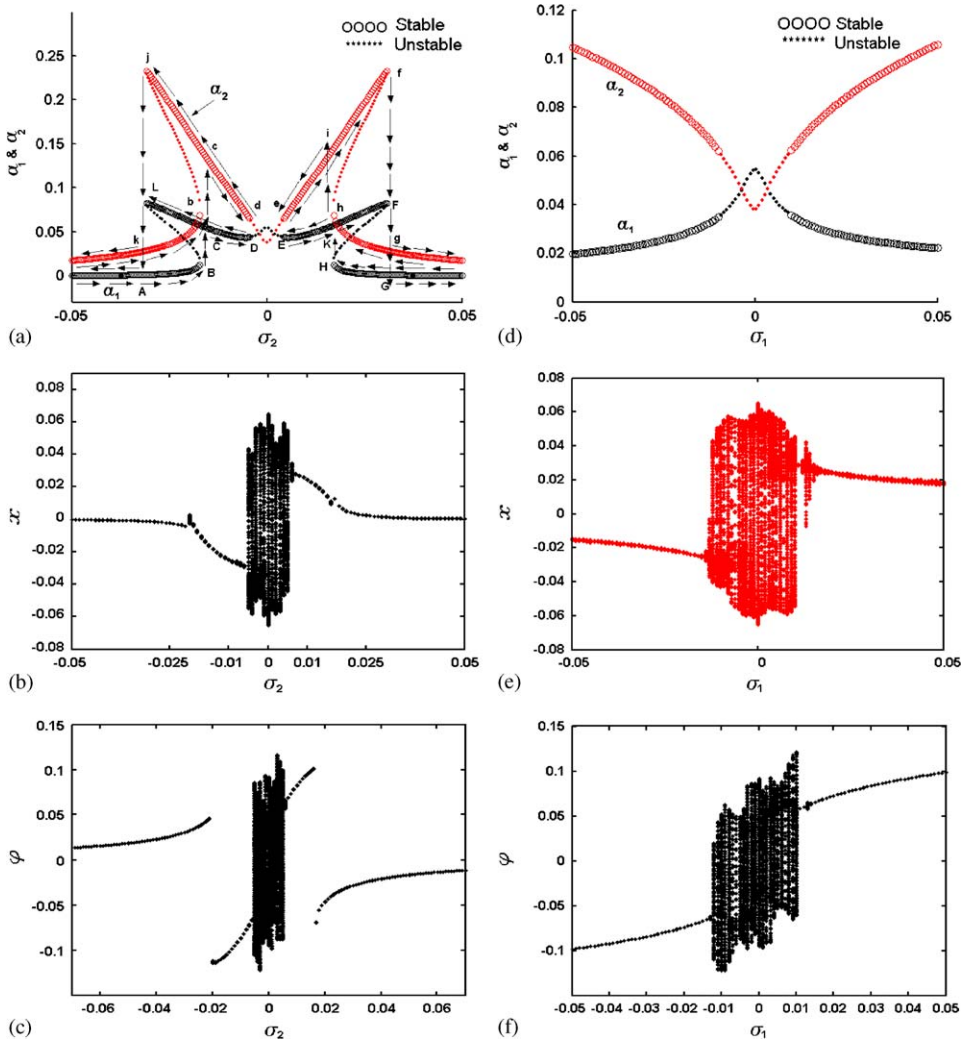

Fig. 9. Frequency response of spring and pendulum modes and associated bifurcation diagrams. (a) Variations of a_1 and a_2 versus σ_2 for $\sigma_1 = 0.0$. (b and c) Bifurcation diagrams of x and φ associated with '(a)'. (d) Variations of a_1 and a_2 versus σ_1 for $\sigma_2 = 0.0$. (e and f) Bifurcation diagrams of x and φ associated with '(d)'.

these basins indicate fractal behavior, as shown in magnification projection window in Fig. 8b.

4.2. *Pendulum mode excitation:* ($\Omega \approx \omega_2$, $f_1 = 0$)

Now consider the evolution of solution for $\omega_2 = 0.5$ and $f_2 = 0.00087$ as functions of detuning parameters (σ_1 and σ_2) and damping coefficients (c_1 and c_2). In Fig. 9a, a_1 and

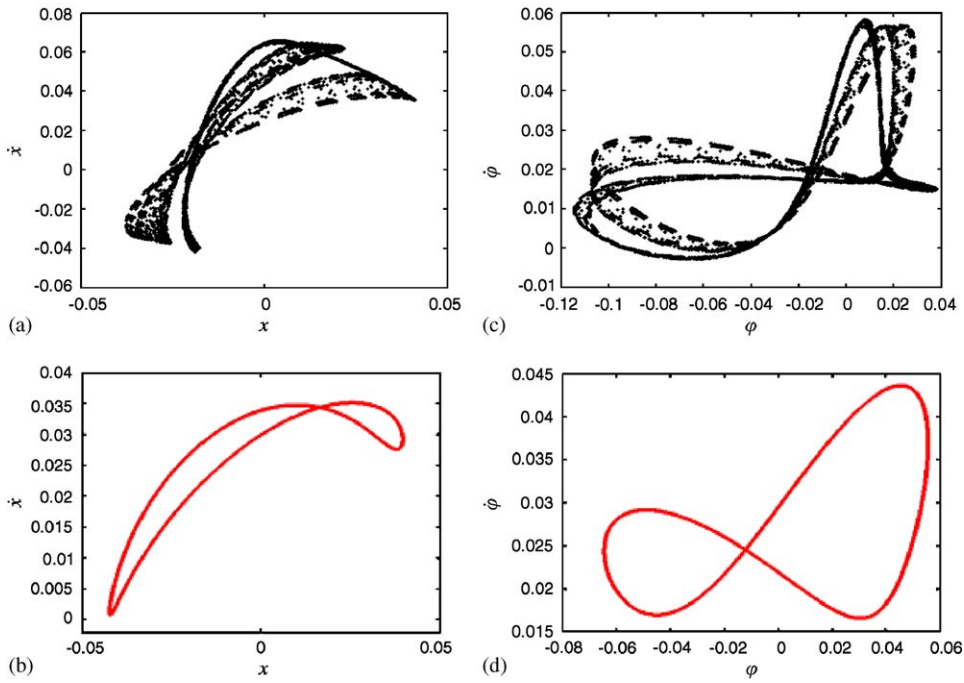

Fig. 10. Poincaré maps for (a) chaotic response of spring mode for ($\sigma_1 = -0.01$, $\sigma_2 = 0.005$, $c_1 = c_2 = 0.005$), (b) quasi-periodic response of spring mode for ($\sigma_1 = 0.0$, $\sigma_2 = 0.001$ $c_1 = 0.01$, $c_2 = 0.005$) (c) chaotic response of pendulum mode associated with '(a)' and (d) quasi-periodic response of pendulum mode associated with '(b)'.

a_2 are plotted as functions of σ_2 for $\sigma_1 = 0$ and $c_1 = c_2 = 0.005$. The jump phenomena are indicated by arrows. As σ_2 increases, a_1 moves from A to B and then jumps up from B to C and then moves along CDEF. As σ_2 increases to the right of F, a_1 jumps down from F to G. Similar jumps occurred when σ_2 decreases from G. Jumpings up and down of a_2 solution are also shown by arrows. In Fig. 9d, a_1 and a_2 are plotted as functions of σ_1 for $\sigma_2 = 0$ and $c_1 = c_2 = 0.005$. In this case it is shown that neither a_1 nor a_2 jumps.

The important phenomenon that observed in Fig. 9, is the unstable periodic motion of both modes for some values of σ_1 and σ_2. Constructing the bifurcation diagrams of x and φ, it is observed that the solutions are bounded but not periodic (Fig. 9b,c, and e,f).

The non-periodic regions are also examined by constructing the Poincaré map of solutions for special values of parameters that are shown in Fig. 10. In most points of the unstable periodic regions, it is seen that the solutions are quasi-periodic (Fig. 10b and d) and only in special cases the chaotic solutions may occur (Fig. 10a and c).

Amplitudes of spring and pendulum modes, a_1 and a_2, are plotted versus to the amount of external detuning parameter σ_2 in Fig. 11. In this plot the internal detuning parameter has been set to $\sigma_1 = -0.001$. Comparing Figs. 9a and 11, one can say that the positive and negative values of σ_1 pulls the frequency response of a_1 and a_2 to the right (hard spring) and left (soft spring), respectively.

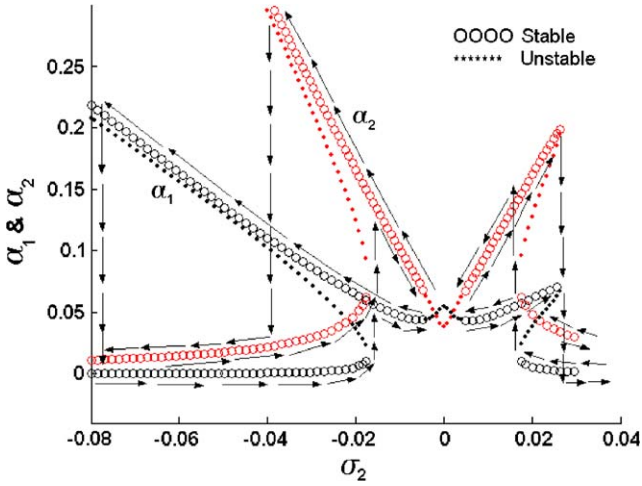

Fig. 11. Frequency response of spring and pendulum mode and the effect of σ_1.

In Fig. 12a and b, amplitudes a_1 and a_2 are plotted as functions of σ_2, respectively, for $\sigma_1 = 0$ and $c_2 = 0.005$, and various values of c_1. Also in Fig. 12c and d, for $c_1 = 0.005$ and various values of c_2, a_1 and a_2 are plotted as functions of σ_2, respectively. Fig. 12 shows the influence of damping coefficients on the steady state solutions. It should be noted that the existence of multiple solution also depends on the damping of modes. For special values of damping coefficients the jumping phenomena is observed. In these figures the extreme sensitivity of a_1 and a_2 to the amount of modal dampings should be noted.

In the case of pendulum mode excitation, the existence of multiple attractors can be detected for both modes, which are shown in Figs. 9a and 12. For example Fig. 9a shows that for both spring and pendulum modes, two stable regular attractors exist in the range of $0.017 < |\sigma_2| < 0.032$. For $\sigma_2 = -0.025$, the stable attractors of pendulum mode are at $a_2 = 0.035$ and 0.195. The basin of attraction for these two attractors, in $(x(0), \varphi(0))$-plane, for $\dot{x}(0) = \dot{\varphi}(0) = 0.0$, and by discretizing the square $[-0.5, 0.5] \times [-0.5, 0.5]$ into a grid of 200×200, is shown in Fig. 13a. In some regions of initial condition space, a fractal pattern similar to that of spring mode excitation can be observed for pendulum mode excitation, Fig. 13b.

5. Conclusion

This paper investigates the response of spring-pendulum system. Although earlier studies show that the response in some regions become unstable, we have shown that there are also the possibility of quasi-periodic and chaotic solutions. Our investigations illustrated that deviation from the internal or external resonances may result in quasi-periodic or chaotic states. We have also shown that the damping variations have significant effects on the steady state system response. For some values of damping coefficients, jumping and chaotic motion

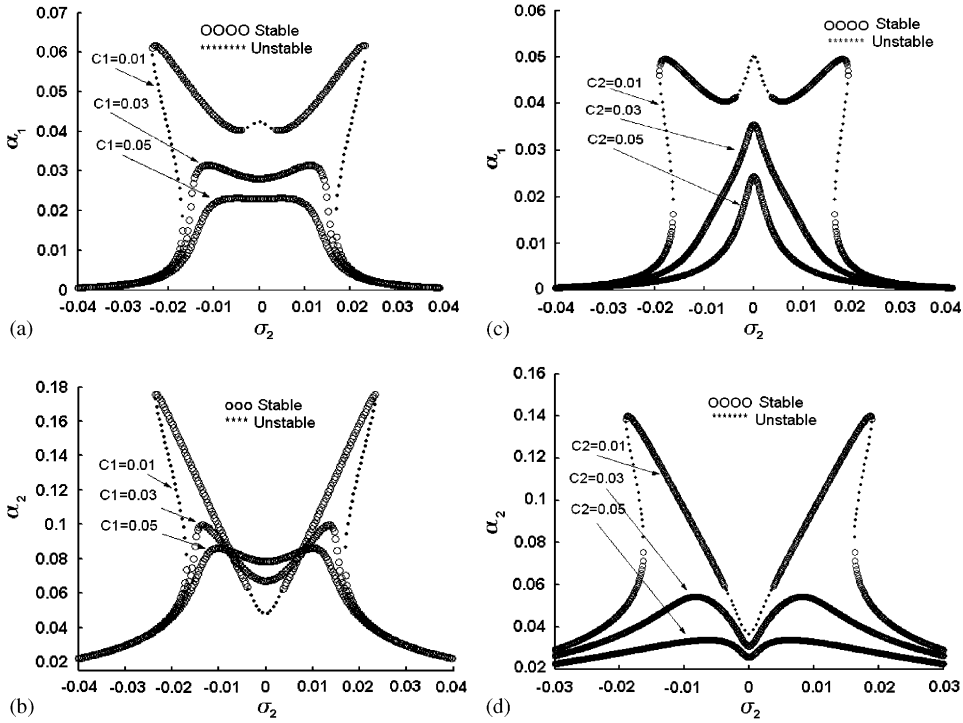

Fig. 12. (a) Spring mode amplitude and (b) pendulum mode amplitude for various value of spring mode damping coefficient ($\sigma_1 = 0.0$, $\sigma_2 = 0.005$). (c) Spring mode amplitude and (b) pendulum mode amplitude for various value of the pendulum mode damping coefficient ($\sigma_1 = 0.0$, $c_1 = 0.005$).

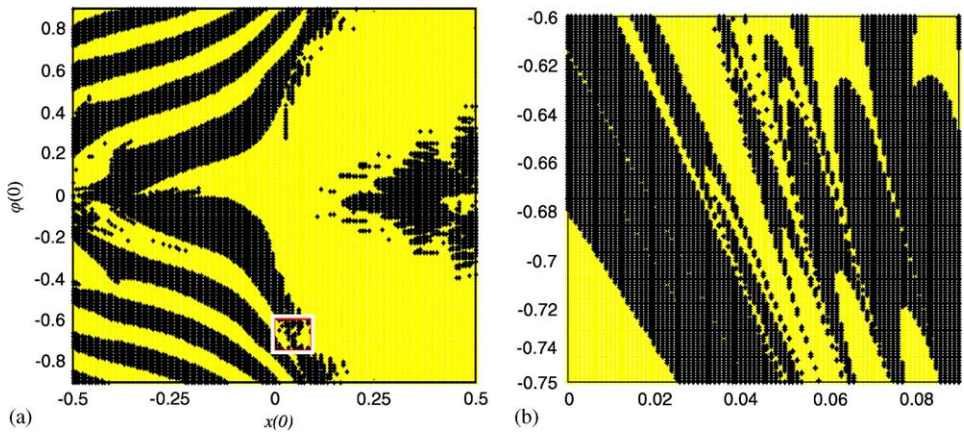

Fig. 13. Basin of attraction diagrams. (a) In ($x(0)$, $\varphi(0)$) plane and (b) Magnification of the region defined by the rectangle in '(a)'.

may also happen. When the system has its own multiple regular attractors, attractive domains associated with different solutions show the fractal basin boundaries. Consequently, the loss of absolute predictability in the face of small uncertainties in initial conditions would happen.

References

[1] A. Agliari, L. Gardini, C. Mira, On the fractal structure of basin boundaries in two-dimensional noninvertible maps, Int. J. Bifurcat. Chaos 13 (7) (2003) 1767–1785.
[2] R. Bhattacharyya, Behavior of a rubber spring pendulum, J. Appl. Mech. 67 (2) (2000) 332–337.
[3] M.T. Defreitas, R.L. Viana, C. Grebogi, Multistability, basin boundary structure, and chaotic behavior in a suspension bridge model, Int. J. Bifurcat. Chaos 14 (3) (2004) 927–950.
[4] A.F. El-Bassiouny, Parametrically excited nonlinear systems: a comparison of two methods, Int. J. Math. Math. Sci. 32 (12) (2002) 739–761.
[5] W. Garira, S.R. Bishop, Oscillatory orbits of the parametrically excited pendulum, Int. J. Bifurcat. Chaos 13 (10) (2003) 2949–2958.
[6] T. Georgiou Ioannis, On the global geometric structure of the dynamics of the elastic pendulum, Nonlinear Dyn. 18 (1) (1999) 51–68.
[7] C. Grebogi, S.W. McDonald, E. Ott, J.A. York, Final state sensitivity: an obstruction to predictability, Phys. Lett. A 99 (9) (1983) 415–418.
[8] C. Grebogi, E. Ott, J.A. York, Fractal basin boundaries, long-lived chaotic transients and unstable–unstable pair bifurcation, Phys. Rev. Lett. 50 (13) (1983) 935–938.
[9] W.K. Lee, C.S. Hsu, A global analysis of a harmonically excited spring-pendulum system with internal resonance, J. Sound Vib. 171 (3) (1994) 335–359.
[10] W.K. Lee, H.D. Park, Chaotic dynamics of a harmonically excited spring-pendulum system with internal resonance, Nonlinear Dyn. 14 (1997) 211–229.
[11] G.X. Li, F.C. Moon, Criteria for chaos of a three-well potential oscillator with homoclinic and hetroclinic orbits, J. Sound Vib. 136 (1) (1990) 17–34.
[12] J. Miles, Resonantly forced motion of two quadratically coupled oscillators, Physica D 13 (1984) 247–260.
[13] F.C. Moon, G.X. Li, Fractal basin boundaries and homoclinic orbits for periodic motions in a two-well potential, Phys. Rev. Lett. 55 (14) (1985) 1439–1442.
[14] A.H. Nayfeh, Parametric excitation of two internally resonant oscillators, J. Sound Vib. 119 (1) (1987) 95–109.
[15] T.A. Nayfeh, W. Asrar, A.H. Nayfeh, Three-mode interactions in harmonically excited systems with quadratic nonlinearities, Nonlinear Dyn. 58 (1991) 1033–1041.
[16] A.H. Nayfeh, B. Balachandran, Experimental investigation of resonantly forced oscillations of a two-degree-of-freedom structure, Int. J. Non-linear Mech. 25 (2/3) (1990) 199–209.
[17] A.H. Nayfeh, B. Balachandran, M.A. Colbert, M.A. Nayfeh, An experimental investigation of complicated response of a two-degree-of-freedom structure, ASME J. Appl. Mech. 56 (1989) 960–967.
[18] A.H. Nayfeh, D.T. Mook, L.R. Marshall, Nonlinear coupling in pitch and roll modes in ship motions, J. Hydronaut. 7 (4) (1973) 145–152.
[19] A.H. Nayfeh, L.D. Zavodney, Experimental observation of amplitude- and phase-modulated response of two internally coupled oscillators to a harmonic excitation, ASME J. Appl. Mech. 55 (1988) 706–710.
[20] P.R. Sethna, Vibrations of dynamical systems with quadratic nonlinearities, J. Appl. Mech. 32 (1965) 576–582.
[21] W. Szemplinska-Stupnicka, E. Tyrkiel, A. Zubrzycki, The global bifurcations that lead to transient tumbling chaos in a parametrically driven pendulum, Int. J. Bifurcat. Chaos 10 (9) (2000) 2161–2175.
[22] S. Tousi, A.K. Bajaj, Period-doubling bifurcations and modulated motions in force mechanical systems, ASME J. Appl. Mech. 52 (1985) 446–452.
[23] K. Zaki, S. Noah, K.R. Rajagopal, A.R. Srinivasa, Effect of nonlinear stiffness on the motion of a flexible pendulum, Nonlinear Dyn. 27 (1) (2002) 1–18.